Bull. Mater. Sci. (2026) 49:19
https://doi.org/10.1007/s12034-025-03538-8

Ultra-wideband absorber design based on Sprott (2014) chaotic system for high-performance microwave applications

MERTCAN ORAL[1], FIKRET ALPAY TEKSEN[1], BERKER COLAK[1], MEHMET BAKIR[2], AHMET SERTOL KOKSAL[2], FARUK KARADAG[3], LULU WANG[4,5] and MUHARREM KARAASLAN[1,*]

[1]Department of Electrical and Electronics Engineering, Iskenderun Technical University, 31200 Hatay, Turkey
[2]Department of Computer Engineering, Bozok University, 66100 Yozgat, Turkey
[3]Department of Physics, Faculty of Art and Sciences, Cukurova University, 01330 Adana, Turkey
[4]Department of Engineering, Reykjavik University, 102 Reykjavik, Iceland
[5]College of Science, Engineering and Technology, University of South Africa, Midrand, Gauteng 1686, South Africa
*Author for correspondence (muharrem.karaaslan@iste.edu.tr)

MS received 27 May 2025; accepted 18 September 2025

Abstract. This study presents an analysis of the Sprott (*Phys. Lett. A* **378** 1361–1363, 2014) chaotic patterned electromagnetic absorber, which exhibits a broadband band absorption rate in the range of 2–20 GHz. The application studies commenced with an analysis of the parameters of the Sprott (2014) chaotic attractor, resulting in the generation of three-dimensional plane images. Given that the z-plane has a standard thickness of 0.035 mm in the electromagnetic absorber to be designed, the three-dimensional images obtained were processed with various iterations in the Julia fractal and transformed into two-dimensional patterns. These patterns were then examined in the simulation environment to assess the electromagnetic absorption of the patterns. In the design of the electromagnetic absorber, the chaotic patterns have been defined as copper with a standard thickness of 0.035 mm, and Magtrex 555, which exhibits frequency-dependent permeability, was selected as the substrate. In order to achieve the maximum absorption value, the back layer of the electromagnetic absorber structure was coated with copper sheet. This study examines the impact of the design parameters, including substrate thickness, absorber size, and substrate type, on the absorption rate of the electromagnetic absorber through a parametric analysis. The operational methodology of the proposed structure was elucidated through an examination of the electric field and surface current distributions at various resonant frequencies. The characteristics of the Sprott (2014) chaotic patterned electromagnetic absorber were subjected to a comprehensive analysis, which reveals its potential for integration into a multitude of contemporary applications. Notably, this study marks the inaugural application of the Sprott (2014) chaotic method in the design and optimization of a metamaterial absorber, thereby contributing a novel perspective to the existing literature on the subject.

Keywords. Sprott (2014) chaotic attractor; electormagnetic absorber; pattern recognition; image generation.

1. Introduction

The utilisation of microwave devices across a multitude of disciplines is witnessing a marked increase on a daily basis. As the use of microwave devices continues to grow, a number of issues have emerged, including interference and poor performance. In response, microwave absorbers have been developed with the aim of reducing interference, undesired reflections, radar cross-sectional areas and improving the performance of microwave devices [1]. The high absorption efficiency of microwave absorbers across a wide frequency range makes them an effective solution to these problems. They are used in a range of fields, including military, health and communication [2–8]. Conventional electromagnetic absorber designs have typically been composed of periodic structures or multilayer configurations. However, in response to the growing demand for smaller and more efficient designs, new approaches are being explored with the aim of achieving enhanced performance across a wider frequency range.

An innovative approach in this field is the application of chaotic patterns generated by chaotic attractors in microwave absorber design [9–11]. The distinctive potentialities of chaotic systems, which exhibit a proclivity for sensitive dependence on initial conditions and non-periodic behaviour can be harnessed to construct intricate and broadband absorption surfaces [12,13]. Among low-dimensional chaotic flows, three-dimensional systems are particularly attractive for geometry generation because they combine analytical simplicity with rich, parameter-dependent

Published online: 24 January 2026

dynamics and highly irregular but deterministic trajectories. Such properties make them well suited for producing geometrically intricate, scalable patterns amenable to electromagnetic design [14–16]. In this work, we specifically adopted the time-reversible three-dimensional system introduced by Sprott (2014) [17], which exhibits sensitive dependence on initial conditions and supports qualitatively distinct behaviours under different conditions, and we used it as the chaotic driver in our chaos-to-fractal mapping pipeline.

This study proposes a microwave absorber with high absorption values operating in the ultra-wide bandwidth range based on the Sprott (2014) chaotic attractor. The Sprott (2014) chaotic pattern microwave absorber has been designed to operate with optimal efficiency in the frequency range of 2–20 GHz. In order to create the chaotic patterns, three-dimensional trajectories obtained from the Sprott (2014) chaotic attractor were utilized. These trajectories are transferred to the Julia fractal set of fractal geometry tools, and the Sprott (2014) chaotic trajectories obtained by applying iterations are optimized and converted into two-dimensional chaotic patterns, which are subsequently applied to the microwave absorber.

In this study, the Rogers Magtrex 555 laminate was identified as the optimal substrate for the proposed microwave absorber, and its absorption performance was evaluated in comparison with a range of alternative substrates. Furthermore, the effects of varying substrate thickness, unit cell size, different chaotic parameters, different operating modes, and angular dependencies were investigated through parametric studies, and the electric field and magnetic field distribution of the structure at various frequencies were analyzed. The proposed structure has thus demonstrated an absorption rate above 90% in the frequency range of 2–20 GHz. This study demonstrates the successful utilization of chaotic structures in a variety of microwave applications, particularly in the field of electromagnetic absorbers.

2. Materials and methods

2.1 *Pattern generation process using the Sprott (2014) chaotic system*

Following Sprott (2014) [X1], we employed a three-dimensional, time-reversible chaotic flow written in parametric form as:

$$\dot{x} = y + axy + xz$$
$$\dot{y} = 1 - bx^2 + yz$$
$$\dot{z} = x - x^2 - y^2 \quad (1)$$

where a and b are control parameters. Unless otherwise stated, we refer to this model as the Sprott (2014) system and use it as the chaotic driver for our chaos-to-fractal mapping pipeline that generates absorber geometries.

2.2 *Parameter exploration and numerical setup*

In this study, the control parameter a was systematically varied in the range $0.05 \le a \le 3.0$ (step size 0.05) to explore regions of chaotic dynamics, while b was fixed at $b = 1.0$. Numerical solutions were obtained using Euler's method with a step size $h = 0.08$. The initial conditions were chosen as $x(0) = 0.87$, $y(0) = -0.51$ and $z(0) = -0.76$, which are known to yield chaotic trajectories within this parameter regime. Visual outputs were generated at a resolution of 480 × 480 pixels, and the resulting attractor shapes were evaluated for absorber design. Among the tested configurations, the most suitable patterns for microwave absorber geometry emerged when $a = 1.65$ (with $b = 1$). The corresponding phase-space trajectories of the Sprott (2014) system, projected along the x-, y- and z- axes, are illustrated in figure 1a–d.

2.3 *Normalization*

To bound each chaotic time series within a fixed numeric range while preserving its temporal shape, we applied component-wise peak (L_∞) normalization. For each coordinate component $u \in \{x(t), y(t), z(t)\}$, we define

$$M_u = \max_t |u(t)|. \quad (2)$$

The normalized series to adjust the geometric resolution is then given by

$$\hat{u}(t) = K \frac{u(t)}{M_u} \quad (3)$$

which guarantees $\sup_t |\hat{u}(t)| = K$ (i.e., $\hat{u}(t) \in [-K, K]$). The factor K was used to adjust the geometric resolution of the generated patterns. Because scaling is performed separately for each component, the aspect ratio of the (x, y, z) projection was allowed to change; this was intentional for our design pipeline. For downstream steps we simply used the normalized variables,

$$[x(t), y(t), z(t)] \leftarrow [\hat{x}(t), \hat{y}(t), \hat{z}(t)] \quad (4)$$

2.4 *Julia set transformation (chaos-to-fractal mapping)*

Using the $\hat{x}(t)$ and $\hat{y}(t)$, we constructed a 480 × 480 complex field and iterated utilizing a quadratic Julia set mapping. Let $\{x[i]\}_{i=1}^{480}$ and $\{y[j]\}_{j=1}^{480}$ be uniformly sampled values from the normalized coordinate ranges. For each pixel point (p, q) in raster order (left-to-right, top-to-bottom), the initial complex value is defined as follows:

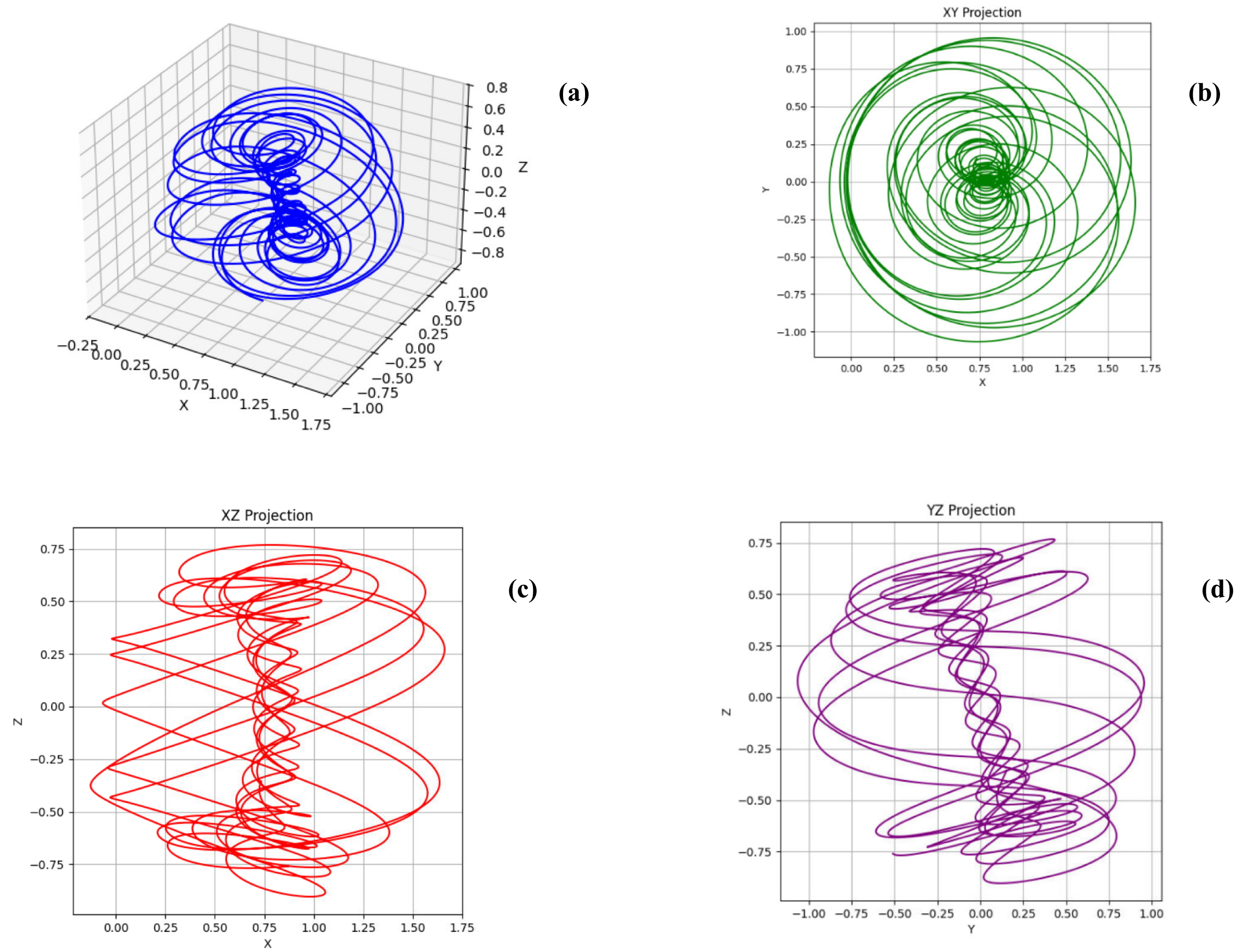

Figure 1. The phase space trajectory of the Sprott (2014) chaotic system illustrated in (**a**) xyz, (**b**) xy, (**c**) xz and (**d**) yz projections.

$$w_0^{(p,q)} = x[p] + iy[q], p, q \in \{1, \ldots, 480\} \tag{5}$$

A classical Julia iteration is then applied [18]:

$$w_{n+1}^{(p,q)} = \left(w_n^{(p,q)}\right)^2 + k, k = -0.175 + 0.655i, n = 0, \ldots, \text{MaxIter} \tag{6}$$

with MaxIter = 100. Coloring is determined by an escape-time rule: the pixel value is mapped to the smallest n for which

$$\left|w_n^{(p,q)}\right| > \tau, \text{where } \tau = |K + k|; \tag{7}$$

otherwise the MaxIter value is assigned. This choice couples the chaotic scaling factor K (from normalization) with the Julia parameter k, yielding a consistent threshold across the image and producing high-complexity, fabrication-ready fractal patterns. This modified Julia mapping thus converts the chaotic trajectories into fractal geometries that serve as candidate absorber patterns.

2.5 *Smoothing, binarization and artefact removal*

The resulting 480 × 480 grayscale image was processed using a two-dimensional Gaussian filter to smooth edges and suppress noise. The filter kernel is given by [19]:

$$G_\sigma(x, y) = \frac{1}{2\pi\sigma^2} \exp\left(-\frac{x^2 + y^2}{2\sigma^2}\right) \tag{8}$$

where σ denotes the standard deviation ($\sigma = 4$ in our experiments). The filtered image was then binarized, and connected component analysis was applied to remove small artefacts. Features with an area smaller than 128 pixels were eliminated, ensuring that the final binary mask retained only physically meaningful absorber geometries suitable for fabrication.

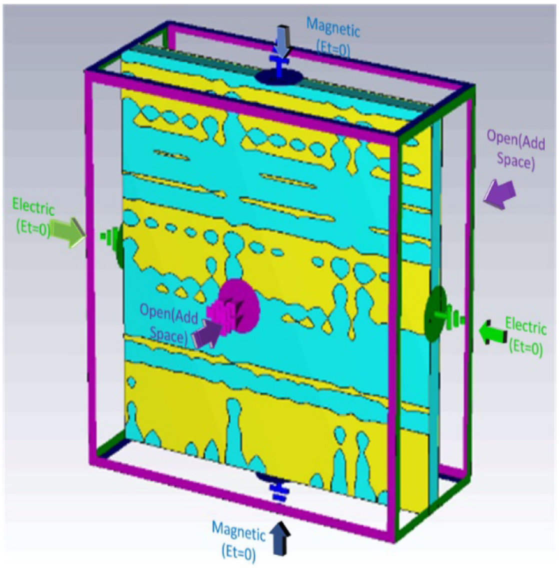

(a)

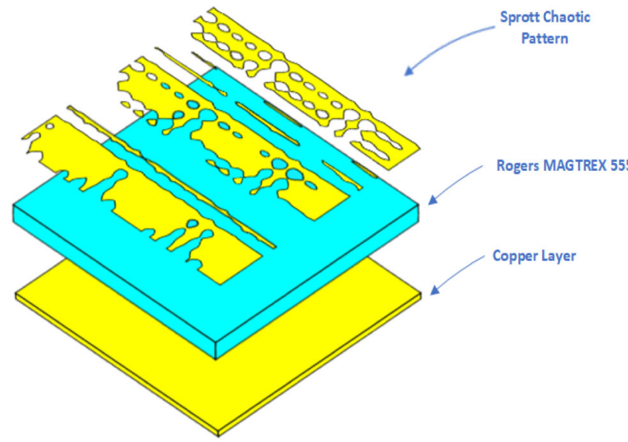

(b)

Figure 2. Setting up boundary conditions for the (**a**) chaotic patterned microwave absorber and (**b**) layers of chaotic microwave absorber.

3. Design and analysis of Sprott (2014) patterned microwave absorber

The essential feature of the chaotic nature of the structures is contingent upon the nonlinear behaviour of the Sprott (2014) system. The algebraic simplicity of three-dimensional ordinary differential equations with Sprott (2014) chaotic solutions precludes the system from attaining periodic or steady states, thereby instigating chaos through the generation of requisite complexity. At this stage of the study, the chaotic patterned image was imported and subjected to analysis within the Finite Integration Based Simulator. This process was carried out in order to investigate the design and performance of the microwave absorber in the related frequency range.

The proposed chaotic patterned absorber was constructed from three distinct parts: a back section coated in copper, a dielectric substrate section, and a chaotic front section with a resistance of 50 Ω/m^2. The size width and height of the absorber structure were Hs = 35 mm. The dielectric substrate layer were elected as Rogers Magtrex 555, with a thickness of 2 mm and a relative permittivity of 5.3 [20]. The absorption is calculated as

$$R = \left|\frac{Z - Z_0}{Z + Z_0}\right|^2 = \left|\frac{\sqrt{\mu_r} - \sqrt{\varepsilon_r}}{\sqrt{\mu_r} + \sqrt{\varepsilon_r}}\right|^2 \quad (9)$$

where Z and Z_0 denote impedance of the metamaterial and free space, respectively.

$$\mathrm{A}(\omega) = 1 - \mathrm{R}(\omega) - \mathrm{T}(\omega) \quad (10)$$

$$A = 1 - R = 1 - \left|\frac{Z - Z_0}{Z + Z_0}\right|^2 = \frac{2\sqrt{\mu_r}\sqrt{\varepsilon_r} + (\mu_r - \varepsilon_r)}{\left(\sqrt{\mu_r} + \sqrt{\varepsilon_r}\right)^2} \quad (11)$$

In equation (10), T(ω) represents transmission and R(ω) represents reflection coefficients. When expressed as frequency-dependent S-parameters, T(ω) is equal to the square of $S21$(ω) and R(ω) is equal to the square of $S11$(ω). Furthermore, given that the rear ground section of our absorber structure is copper, $S21$(ω) value will exhibit values close to 0 within the frequency range under investigation. The boundary conditions Et=0 and Ht=0 are defined in the X- and Y-directions, while the Z-direction is designated as open (figure 2a). The absorption and performance of the microwave absorber were examined within the frequency range of 2–20 GHz. The layers of the microwave absorber are demonstrated in figure 2b.

Figure 3 illustrates the resistance (R), capacitance (C) and inductance (L) components associated with the aforementioned segments. Furthermore, eight capacitors were incorporated into the model to represent the capacitive effects between the segments. The values of all components employed in the design were determined through the application of machine learning techniques and estimation methods. The Advanced Design System (ADS) software was instrumental in this process, facilitating the determination of the optimal value for each component. The application of machine learning enabled the expeditious and precise calculation of the intricate relationships

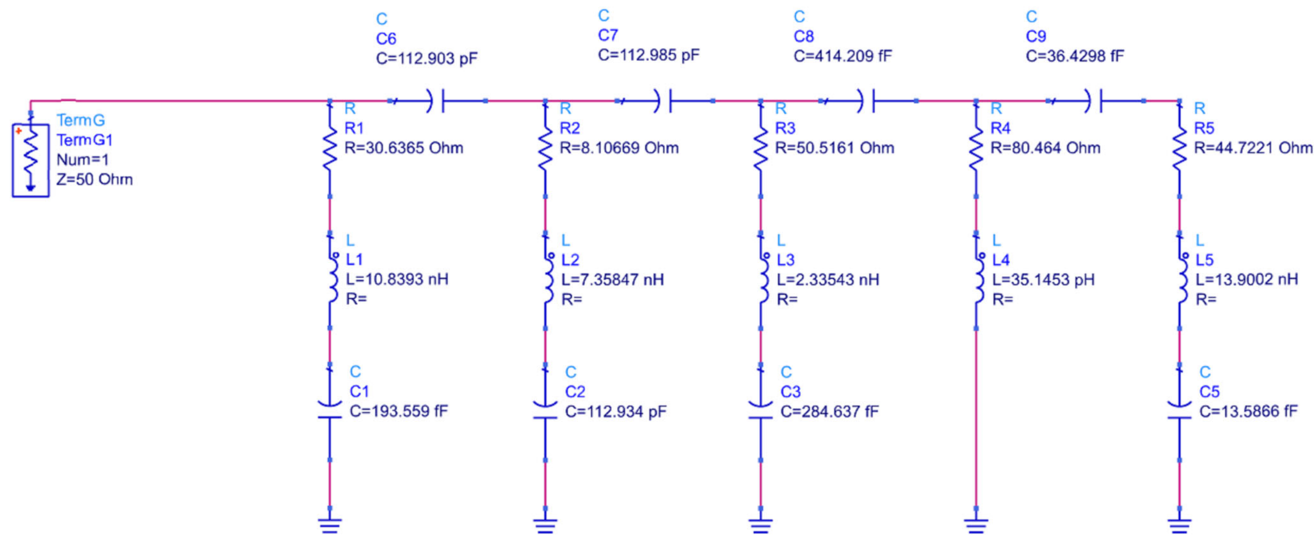

Figure 3. The equivalent circuit representation of the absorber obtained by ADS software.

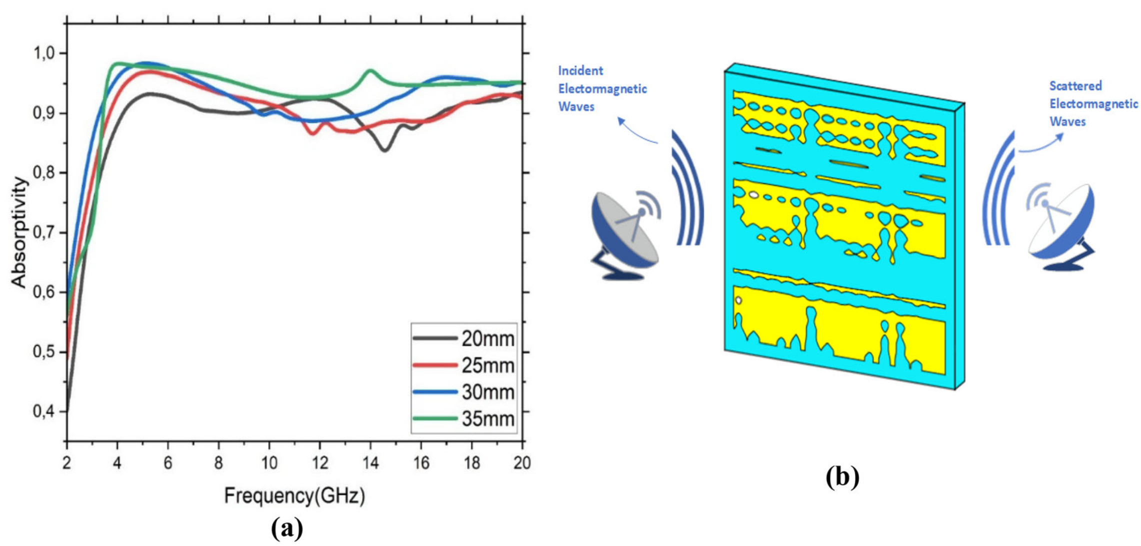

Figure 4. Parametrical studies for absorptivity of the microwave absorber for unit cell dimension (**a**) and the overall structure under test (SUT) (**b**).

and parameters inherent to this circuit design. Each element of the design was optimized to maximize absorption performance. Resistance and inductance values were defined by material properties and geometrical structure, while interactions between capacitors contributed to the enhancement of absorption performance.

4. Numerical results and parametric analysis of the absorptivity of microwave absorber response between 2 and 20GHz

This section presents the findings of an investigation into the performance of a chaotic microwave absorber designed through the application of parametric studies. The primary objective of the investigation is to achieve broadband (2–20 GHz) absorption above 90%. In the initial parametric study, the edge length parameter of the designed microwave absorber was examined by increasing the edge length parameter from 20 to 35 mm in increments of 5 mm. The examination revealed that the structure with an edge length of 35 mm exhibited the most broadband absorption, exceeding 90% in the range of 3–20 GHz, in comparison to the other structures (figure 4a). In the other structures, the absorption decreased below 90% in various frequency ranges, with the lowest absorption observed with an edge length of 20 mm. The outcomes of the parametric studies, conducted with varying edge lengths and unit cell, are illustrated in figure 4a and b.

Furthermore, parametric studies were conducted on the proposed microwave absorber in accordance with the thicknesses of the middle layer (substrate) structures

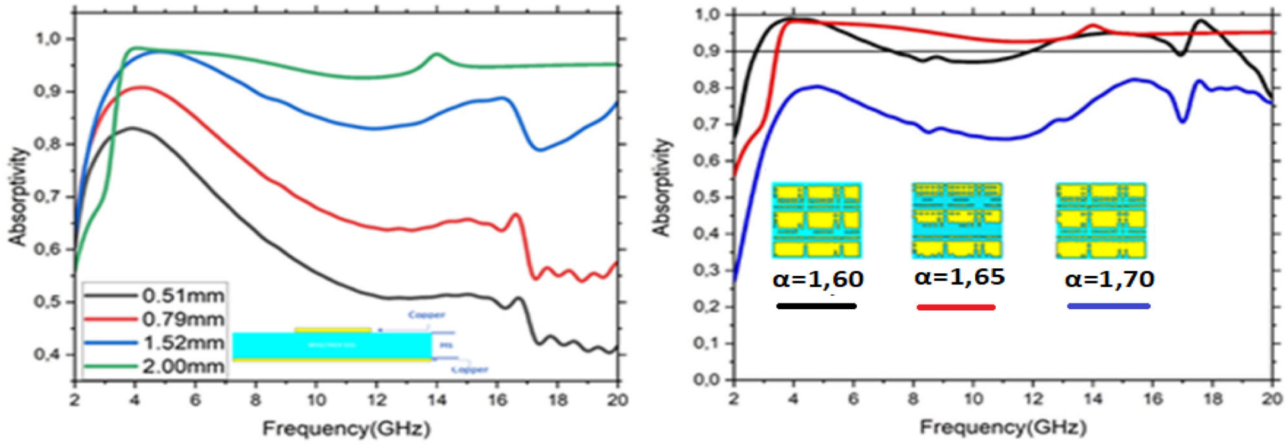

(a) **(b)**

Figure 5. Parametrical studies of the response of microwave absorber for (**a**) thickness and (**b**) parameters**.**

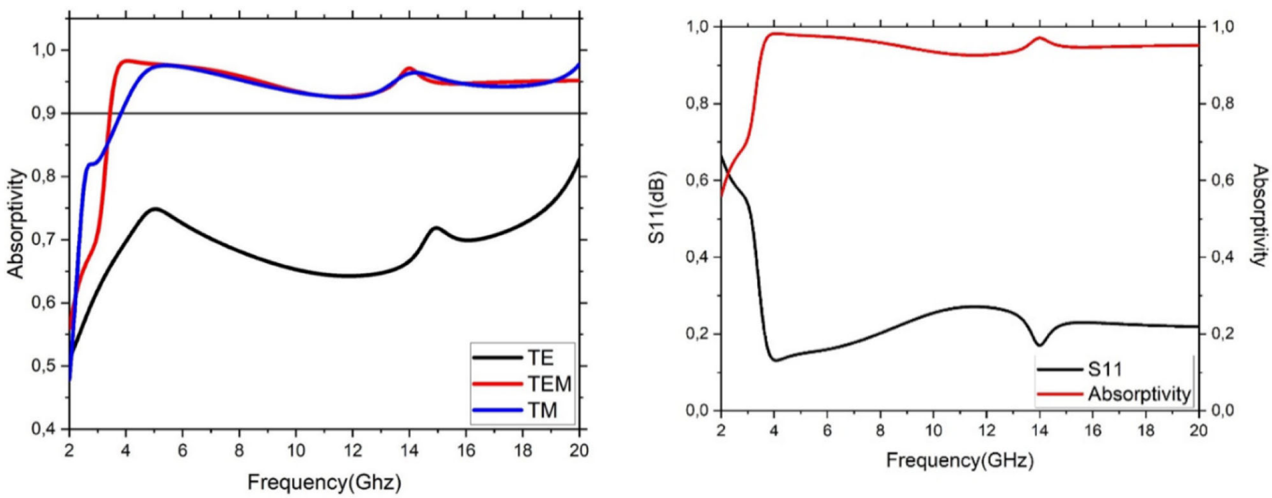

(a) **(b)**

Figure 6. (**a**) Abosorption rates of the microwave absorber for TE, TM and TEM modes. (**b**) S11 and absorption graph of suggested Sprott (2014) chaotic patterned microwave absorber.

currently available on the market. The effect of the thickness of the substrate structures (Hs) on absorptivity was analysed in increments of 0.51 mm, 0.79 mm, 1.52 mm and 2 mm, respectively (figure 5a). The 0.51-mm-thick structure exhibited the highest absorption, reaching 80–82% in the 3–5 GHz range. The highest absorption is observed for 0.79-mm-thick structure, reaching 90–91% in the range of 3.8–4.5 GHz. For the structure with a thickness of 1.52 mm, absorption rates between 90–96% have been observed in the range of 3.6–8 GHz. The structure with a thickness of 2 mm exhibits an absorption rate of 90–98% in the range of 3.6–20 GHz, representing the optimal absorption rate among all thickness parameters. The observed trend of increasing absorption with substrate thickness can be attributed to the enhanced impedance matching and increased path length for the electromagnetic waves within the absorber. Thicker substrates allow more efficient energy dissipation by facilitating stronger interaction between the electromagnetic waves and the absorber material. Additionally, the increased thickness broadens the operational bandwidth by providing a more gradual transition between free space impedance and the absorber's impedance. The outcomes of the parametric studies, conducted with varying thickness, are illustrated in figure 5.

Moreover, the effect of the chaotic control parameter α on the design and absorptionis analysed parametrically. Figure 5b illustrates the impact of the chaotic control parameter α. P at values of 1.60, 1.65 and 1.70, respectively.

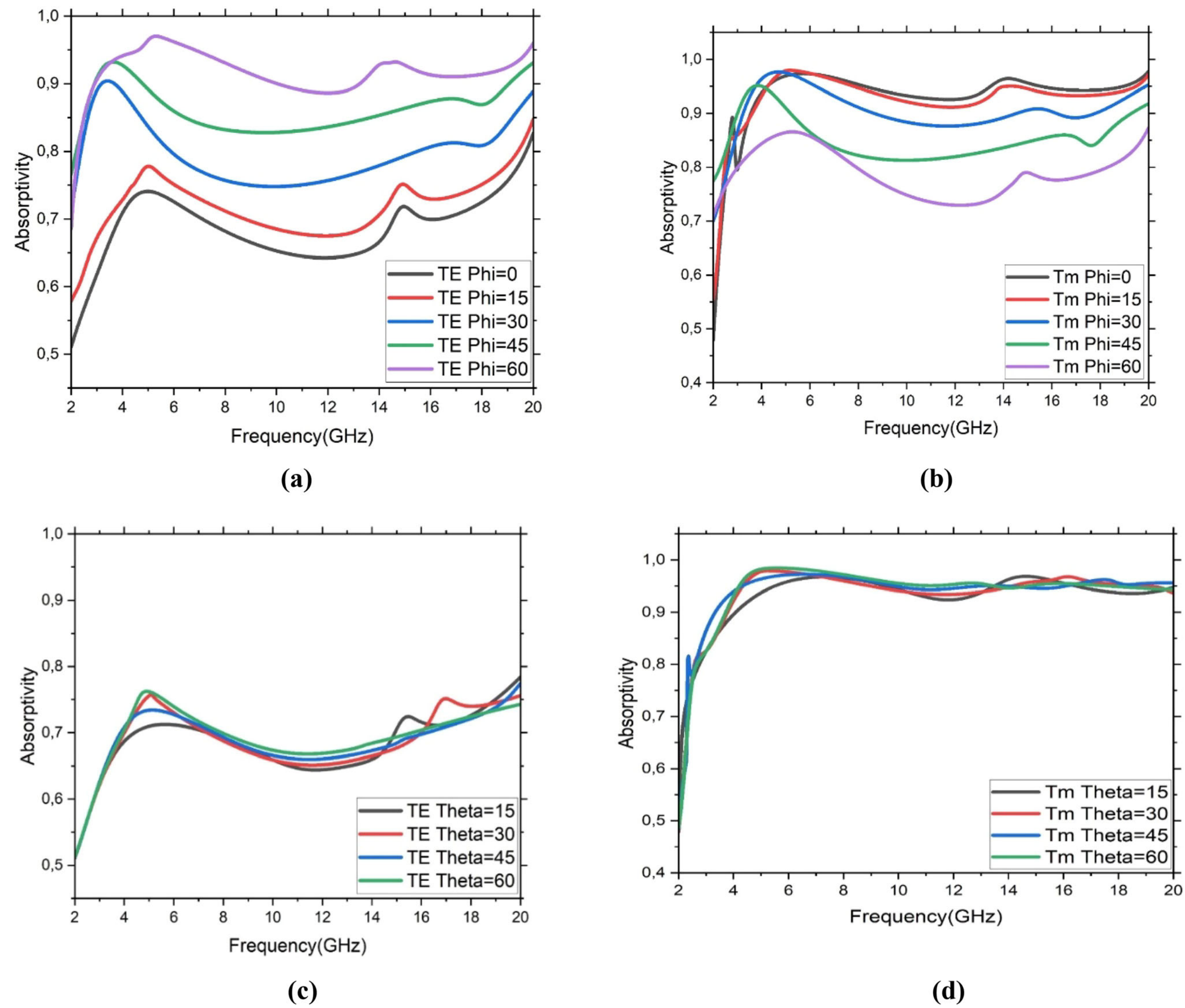

Figure 7. Parametric study of the variation of the polarisation angle phi for the designed microwave absorber in (**a**) TE and (**b**) TM modes. Parametric study of the variation of the incidence angle theta for the designed microwave absorber in (**c**) TE and (**d**) TM modes.

As illustrated in figure 5b, the optimal operating parameter for the chaotic control parameter α is 1.65. In particular, when the value of α is set to 1.70, the absorption decreases significantly, from 90 to 68%. When the chaotic control parameter α is set to 1.60, the suction does not reach α critical point of decrease, but rather exhibits a downward trend. Ultimately, when the chaotic control parameter α is set to 1.65, the absorption rate remains above 90% across the entire band.

In addition, the outcomes yielded in TE, TM and TEM modes for the optimal absorber configuration identified through prior parametric investigations were subjected to parametric simulation. Upon examination of the results, it was found that the highest absorption values were obtained in the TEM mode. Given that the selected substrate, Rogers Magtrex 555, is a material with magnetic properties, the results obtained in the TM mode were observed to be similar to those obtained in the TEM mode. In contrast, the values obtained in the TE mode exhibited the lowest absorption values. Materials such as Rogers Magtrex 555 were typically optimized in terms of magnetic permeability (μ). Given that the magnetic field exerts a minimal or negligible influence on the structure in TE mode, it is not feasible to leverage the magnetic properties of the material. This elucidates why the absorption values in TE mode are typically low. The parametric studies conducted in different modes are illustrated in figure 6a.

The reflection parameter S11 was obtained using a linear scale and is presented in the graph shown in figure 6b. The S11 data was employed to calculate the absorption spectrum of the designed model. The finalized absorption coefficient is illustrated in figure 6b. The results of the analysis demonstrate that the system provides over 90% absorption across a wide frequency range between 3.6 and 20 GHz.

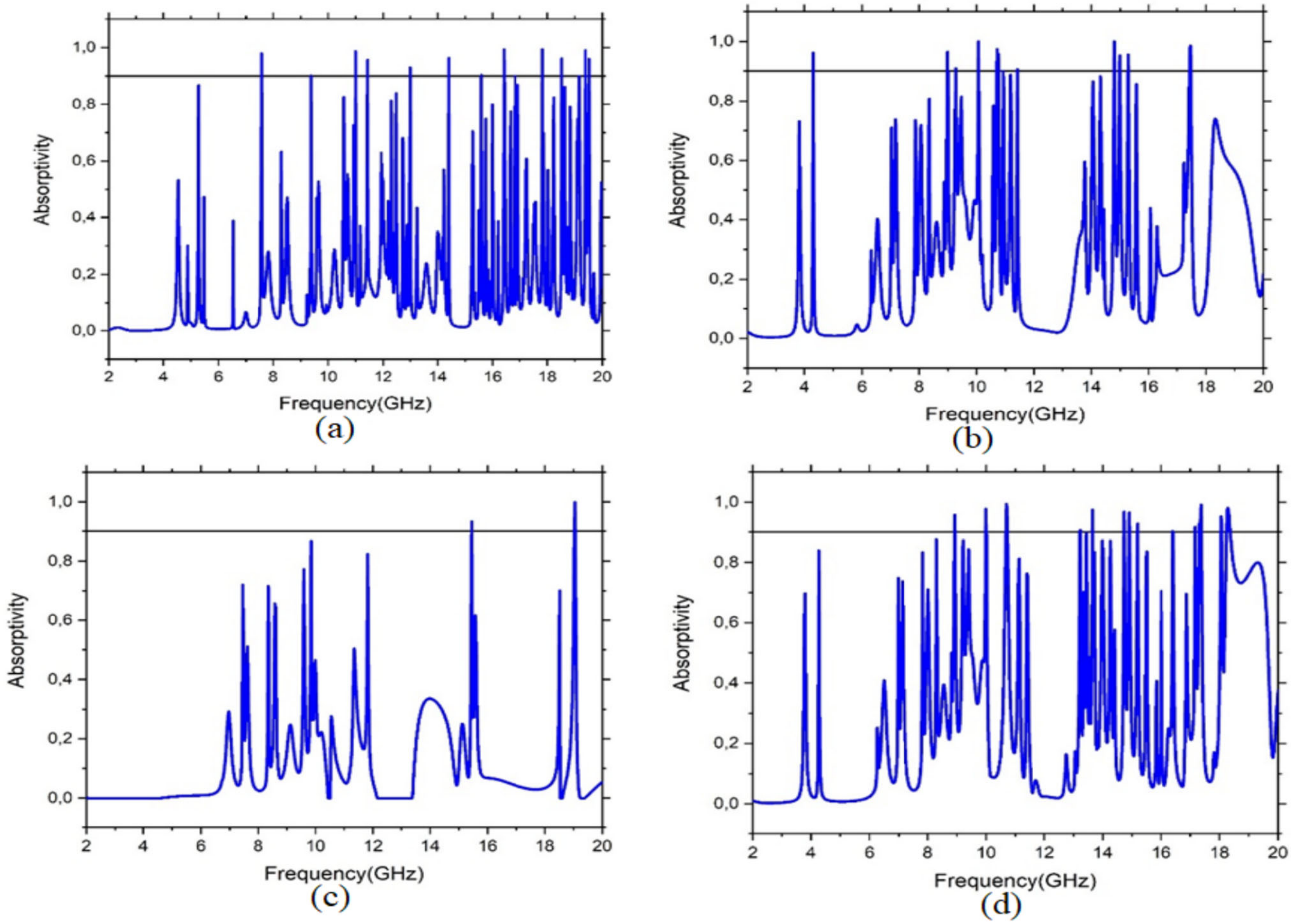

Figure 8. Modelling and absorption graph of chaotic microwave absorber with (**a**) RT/duroid 5880, (**b**) polyamide, (**c**) Rogers RO3003C, and (**d**) Rogers RO4003C.

This broadband absorption performance evinces the efficacy of the designed structure in minimising reflections and enhancing energy absorption within this frequency range. Moreover, a parametric study was undertaken to investigate the impact of the angular dependence of the designed chaotic-patterned microwave absorber on the absorption value, with particular emphasis on the polarisation angle (phi) and the incidence angle (theta). In the study, the angular dependence of the designed chaotic patterned microwave absorber was examined by increasing the theta and phi angles by 15°, and the absorption values in TE and TM modes were evaluated at 0°, 15°, 30°, 45° and 60° incidence angles. It is of paramount importance that the absorber exhibits angular independence, as this guarantees consistent absorption performance under varying electromagnetic wave incidence and polarization angles. This renders it an optimal selection for practical applications where electromagnetic waves may arrive from a multitude of directions and orientations. However, due to the chaotic nature of the design, the absorber does not exhibit complete angular independence. While an increase in the phi angle results in enhanced absorption performance, it remains contingent upon the angle of incidence and polarisation, thereby giving rise to a variation in the absorption values at different angles.

Figure 7a illustrates the impact of varying the phi angle on the TE mode, demonstrating that the lowest absorption values were attained at 0°. It can be concluded that the absorption value increases in accordance with an increase in the phi angle in the TE mode, with the highest absorption values obtained at 60°.

Figure 7b illustrates the variations in the change of the Phi angle in the TM mode. At 0°, the highest rate of absorption is observed, with a subsequent decline in absorption as the angle value increased. The lowest recorded values for absorption are observed at 60°. This behaviour can be attributed to the fact that, in TM mode, the magnetic field vector is oriented in the plane of the structure. As the polarization angle (phi) increases, the alignment between the incident wave's electric field and the absorber's resonant structures becomes less effective, which in turn reduces the efficiency of energy transfer to the absorber. As the phi angle increases, the efficiency of energy transfer to the absorber declines, resulting in a reduction in absorption. Figure 7c illustrates the impact of the theta angle alteration on the absorption values associated with the TE mode

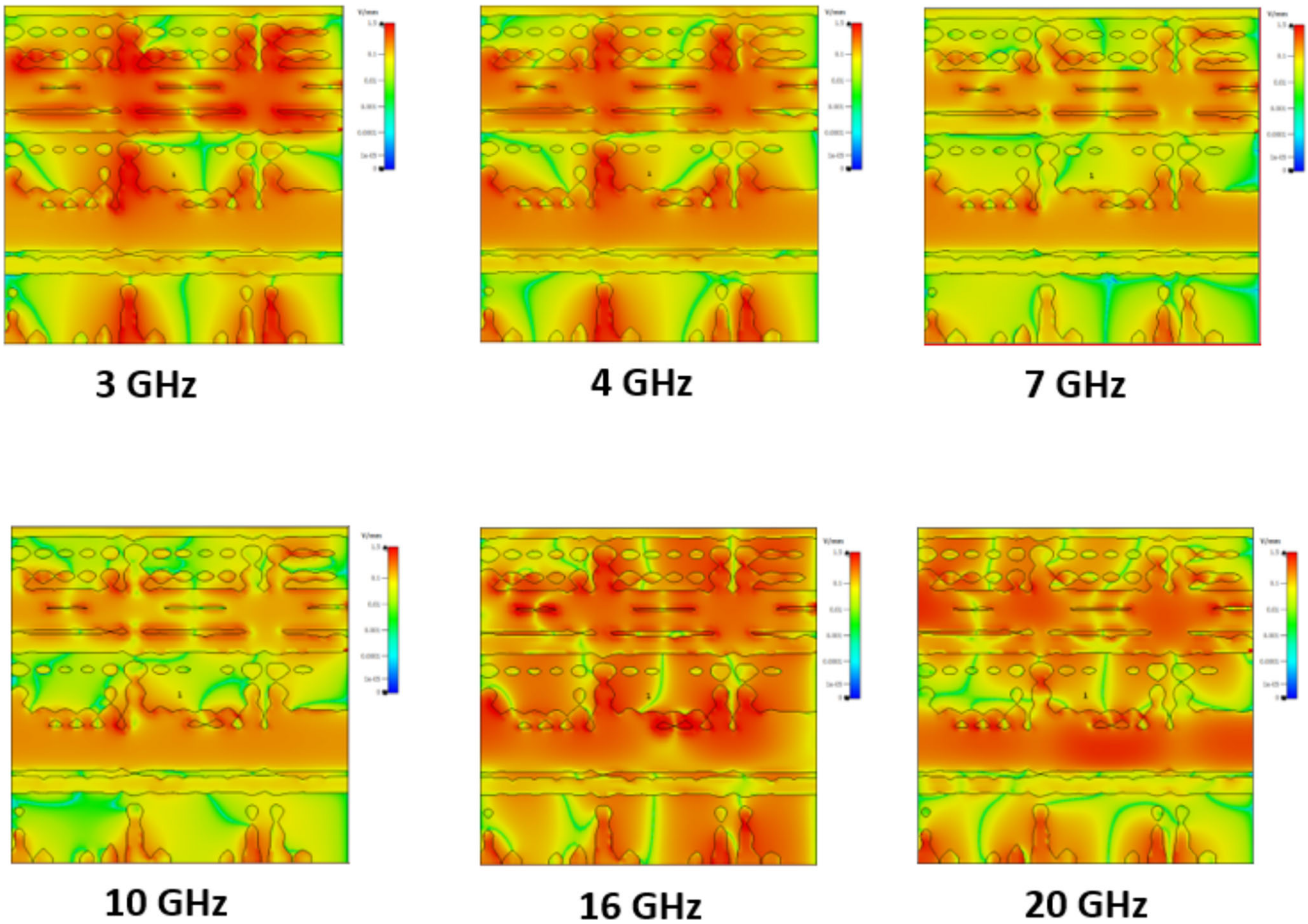

Figure 9. Electric field distributions for resonant frequencies of 3, 4, 7, 10, 16 and 20 GHz.

transition. At the 15° reference point, the lowest absorption values are observed, with an incremental increase in absorption values as the angle increased. While the highest absorption value was attained at 60°, the absorption values recorded for all degrees remained below 90%. Figure 7d illustrates the impact of theta angle alterations on TM mode absorption values. At 15°, the lowest absorption values were observed, while increasing the angle resulted in elevated absorption values. The highest absorption value was attained at 60°. Notably, all absorption values exceeded 90%.

Moreover, parametric studies were conducted to ascertain the influence of the substrate type in the middle layer of the microwave absorber on the absorption rate. The following substrates were employed in the parametric studies: Rogers RT/Duroid 5880 (figure 8a), polyamide (figure 8b), Rogers RO3003C (figure 8c), and Rogers RO4003C (figure 8d). The dielectric constants of these materials are 2.2, 3.5, 3 and 3.55, respectively. Therefore, despite the attainment of considerable absorption rates across all materials, Magtrex 555, which is characterised by frequency-dependent structural parameters, exhibited the highest absorption rates above 90% within the frequency range of 2–20 GHz. The discrepancies in the absorption performance can be ascribed to the dielectric properties of the substrates, most notably their dielectric constants and loss tangents, which impact the impedance matching and energy dissipation characteristics of the absorber. The utilisation of substrates with optimised dielectric constants, such as Magtrex 555, ensures superior impedance matching between the absorber and free space, thereby minimising reflections and enabling efficient wave penetration. Furthermore, the frequency-dependent magnetic properties of Magtrex 555 enhance its capacity to dissipate electromagnetic energy over a broad bandwidth, thereby contributing to its superior absorption performance (figures 8).

The electric field distributions of the designed chaotic patterned microwave absorber at 3, 4, 7, 10, 16 and 20 GHz were also investigated (figure 9). The electric field intensity is represented by a colour scale, whereby high values are represented by red and low values by blue. At 3 GHz, the electric field distribution exhibits a multitude of high-intensity regions, depicted in red and orange, interspersed with low-intensity regions, represented by green and blue. This distribution displays a complex pattern comprising multiple localised centres in the larger-scale portions of the metallic absorber layer. At 4 GHz, the electric field distribution is comparable to that observed at 3 GHz, although

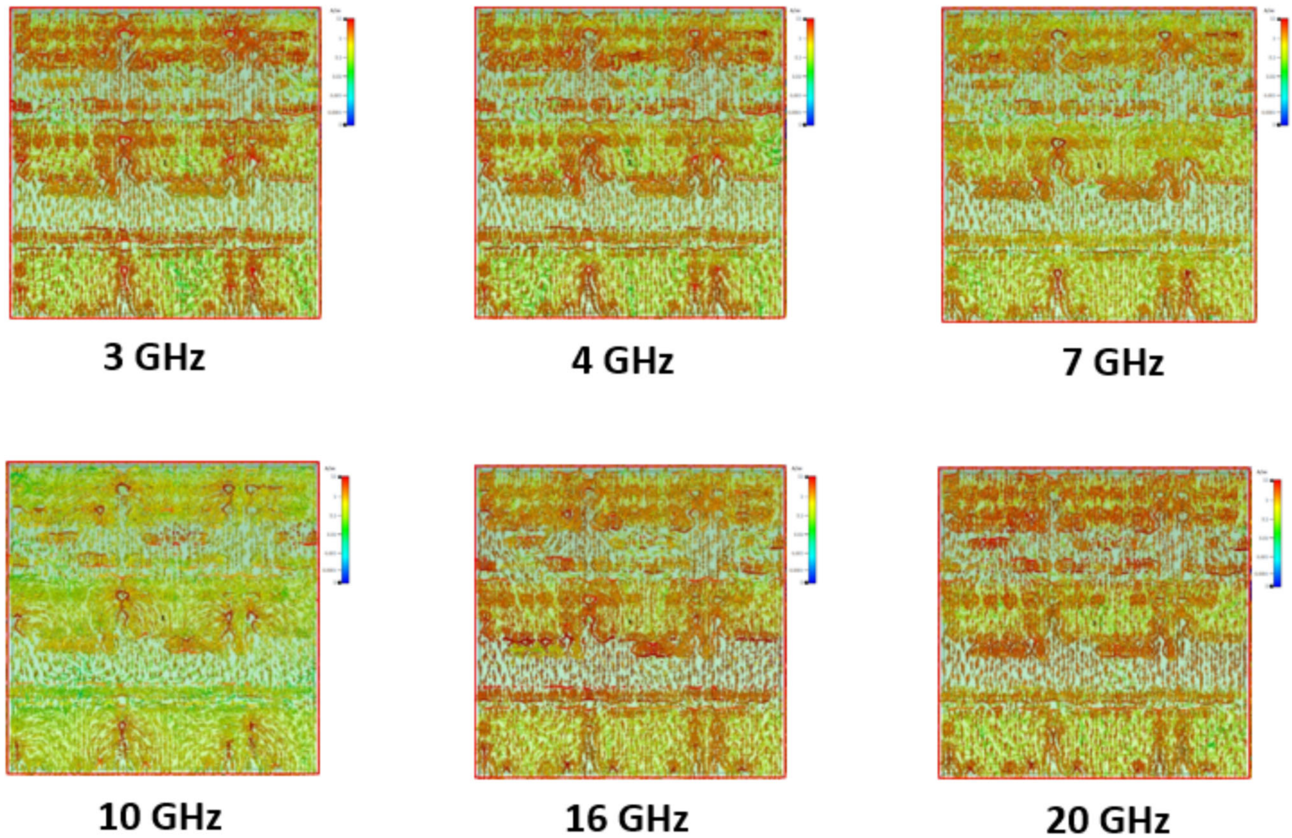

Figure 10. The surface current distributions for resonant frequencies of 3, 4, 7, 10, 16 and 20 GHz.

there are slight differences in the arrangement and intensity of the maximum intensity points. At 7 and 10 GHz, the distributions are similar and, as anticipated, exhibit reduced intensity. At 16 and 20 GHz, the electric field distribution exhibits regions of higher intensity compared to 10 GHz, with the electric field intensity being higher in certain areas, and the red regions becoming more prominent. The electric field distribution varies significantly with higher frequencies tending to show more localised regions of high intensity. Furthermore, the complexity of the electric field patterns increases with frequency, reflecting the interaction between electromagnetic waves and the structure. As a consequence of the electric field distributions, these distributions are related to the resonant modes of the designed absorber structure, material properties and the specific configuration of the electromagnetic system under study.

The surface current distributions of the designed chaotic patterned microwave absorber at 3, 4, 7, 10, 16 and 20 GHz were also investigated. The distributions offer insights into the absorber's performance, elucidating how the surface current density varies as the frequency increases. At lower frequencies (3 and 4 GHz), the surface current distributions are concentrated in specific regions, particularly around the edges of the metamaterial and smaller features. As the frequency increases to 7 and 10 GHz, the surface currents are more evenly distributed over larger regions of the structure. This demonstrates that the chaotic structure exhibits higher resonance at low frequencies (3–4 GHz), lower resonance at medium frequencies (7–10 GHz) than at low frequencies, and higher resonance at high frequencies (16–20 GHz) than at medium frequencies, but lower resonance than at low frequencies (figure 10).

5. Conclusions

This study presents a comprehensive investigation of a microwave absorber design based on the Sprott (2014) chaotic system for a variety of microwave applications. In the course of the research, the three-dimensional graphics generated by varying the parameters of the Sprott (2014) chaotic system were transformed into two dimensions through the Julia Fractal Set, and subsequently included in the simulation analysis. The analyses conducted provided a comprehensive evaluation of the impact of specific design parameters, including side length and substrate thickness, on the absorption properties of the absorber. The findings demonstrate that absorption rates in excess of 90% can be attained within the frequency range of 3.5 to 20 GHz through the implementation of optimised chaotic control parameters. In conclusion, this study demonstrates that chaotic surface-based microwave absorbers have the potential to become a significant alternative for future stealth applications. Furthermore, it highlights that adaptive tuning of the chaotic system parameters presents a crucial avenue for further enhancing the absorption performance.

Although the present study focuses solely on simulation-based results, it should be noted that experimental realisation has not yet been performed. This limitation is mainly due to the high cost and limited availability of the Rogers Magtrex 555 substrate. In our future work, we aim to explore alternative, more accessible dielectric substrates and carry out fabrication and measurement of prototype absorbers to validate the numerical findings.

Acknowledgment

This study was funded by the Scientific and Technological Research Council of Türkiye with grant number of 123F245 scholarship program.

References

[1] Tennant A and Chambers B 2004 *IEEE Microw. Wirel. Co.* **14** 46
[2] Jain P, Chhabra H, Chauhan U, Prakash K, Gupta A, Soliman *et al* 2023 *Sci. Rep. Uk* **13** 1792
[3] Venkatesan R and Singaravelu R 2013 *Proceedings of the Progress in Electromagnetics Research Symposium* (*PIERS*) p 12
[4] Errajraji K, Jebbor N, Das S, Islam T, Madhav B T P and El-Arrouch T 2024 *Opt. Quant. Electron.* **56** 232
[5] Karaaslan M, Bağmancı M, Ünal E, Akgol O and Sabah C 2017 *Opt. Commun.* **392** 31
[6] Zhou B C, Wang D H, Ma J J, Li B Y, Zhao Y J and Li K X 2021 *Waves Random Complex Media* **31** 911
[7] Hossain M B, Faruque M R I, Islam M T, Singh M and Jusoh M 2022 *J. Mater. Res. Technol.* **18** 1653
[8] Sharma A, Singh H and Gupta A 2022 *J. Supercond. Nov. Magn.* **35** 3067
[9] Yuan X, Zhang C, Chen M, Cheng Q, Cheng X, Huang *et al* 2018 *IEEE Antenn. Wirel. Pr.* **18** 197
[10] Zhang R, Ding F, Yuan X and Chen M 2022 *Chin. Phys. Lett.* **39** 094101
[11] Köksal A S and Ünal S 2023 *Phys. Scripta* **98** 115522
[12] Grebogi C, Ott E and Yorke J A 1983 *Physica D* **7** 181
[13] Bakker R, Schouten J C, Giles C L, Takens F and Van den Bleek C M 2000 *Neural Comput.* **12** 2355
[14] Sprott J C 2000 *Am. J. Phys.* **68** 758
[15] Sprott J 2003 *Chaos and Time-Series Analysis*
[16] Hu X, Liu C, Liu L, Ni J and Li S 2016 *Nonlinear Dynam.* **86** 1725
[17] Sprott J C 2014 *Phys. Lett A.* **378** 1361–1363
[18] Julia G 1918 *J. Math. Pure. Appl.* **1** 47
[19] Young I T and Van Vliet L J 1995 *Signal Process* **44** 139
[20] MAGTREX® 555 High Impedance Laminates https://www.rogerscorp.com/advanced-electronics-solutions/magtrex-555-high-impedance-laminates

Publisher's Note